Journal of Rajasthan Academy of Physical Sciences
ISSN : 0972-6306; URL : http://raops.org.in
Vol.15, No.4, December, 2016, 299-313

ON ENTROPY REGIME FOR FLOW AND HEAT TRANSFER OVER A NATURALLY PERMEABLE BED SUBJECTED TO A VARIABLE SUCTION

Paresh Vyas[1] and Swati Soni[2]
Department of Mathematics, University of Rajasthan, Jaipur, India
[1]pvyasmaths@gmail.com
[2]swatisoni19@yahoo.in

Abstract: This communication pertains to entropy generation analysis for the setup comprising flow and heat transfer over a naturally permeable bed subjected to variable suction. A perturbation solution developed for the momentum and energy equations is utilised to compute entropy generation rate. Profiles for the entropy generation number and Bejan number are drawn and discussed.

Keywords: entropy, naturally permeable bed, suction

1. Introduction

Suction plays a vital role in Boundary layer control. Flow and heat transfer in the presence of permeable bed/boundaries is encountered in nature and industrial processes, such as geothermal systems, design of heat exchangers, nuclear waste disposal and thermal insulation applications just to name a few. Porous medium enables to inject or suck out fluid from the system. Vafai and Kim [19], Huang and Vafai [11,12], and Fowler and Bejan [9] have shown that a porous coating/substrate can change the skin friction and temperature gradient at the surface qualitatively and quantitatively. Infact, the porous layer can serve either as an insulater or as a pertinent heat transfer augmentation device. A porous insert has been found to be a pertinent hear augmentation tool.

Flow in the presence of naturally permeable boundary is abundant in nature, for example, natural channels like rivers have gravel beds. We know that the slug flow in a permeable bed is governed by Darcy's law [8], but it is pertinent to note that in the absence of any external pressure gradient and for small permeability the interior flow of the porous medium would not contribute much to the exterior clear fluid flow and therefore zero filter velocity in the permeable bed may be assumed[4]. However, the permeability of the lower bed effects the clear fluid flow through the slip condition suggested by Saffman[18] who showed that for small permeability, the following equation is appropriate to compute the exterior flow correct to $0(K_0)$

$$u = \frac{\sqrt{K_0}}{\alpha}\left(\frac{\partial u}{\partial y}\right)_{y=0^+} + o(K_0)$$

Where u is the fluid velocity, K_0 is the permeability and α is the empirical constant depending upon the porous medium. Entropy generation analysis (EGA) is a pertinent tool for thermodynamic efficiency simply because it serve as a basis for entropy generation minimization (EGM). Last two decades have witnessed great surge for studies on thermofluidic configurations after the pioneer works of Bejan [1-3]. Realising the potential of theoretical second law analysis treatment to thermal processes involving fluid traversal numerous studies appeared in the literature for variety of configurations [5,6,10,13-17,20-24].

The aim of the foregoing problem is to examine the effect of variable suction and permeability on the entropy generation. It is emphasized that no such study on entropy generation has been reported in the literature and it is expected the problem investigated here would be a pertinent introductory endeavour for similarily situated future large scale analogous experimental setups/models where this kind of model is encountered as a single unit or is a part of the setup. The present work is an extension of problem discussed by Chauhan and Sahai [7] where they restricted their analysis to first law of thermodynamics. In this paper, we discuss second law of thermodynamics for the same set up.

2. Formulation of the problem

Let us consider a flow of viscous incompressible fluid over a naturally permeable bed of very small permeability K_0. The bed is subjected to a variable suction. The x-axis is taken along the surface of the permeable bed and y-axis is taken normal to it..Further we assume that the permeable bed is kept at uniform temperature T_0 and the free stream temperature is maintained at uniform temperature T_∞. Considering the permeable bed to be very large, all the parameters except the pressure are independent of x.

The governing equations for the set up are

$$\frac{\partial u}{\partial t} + v\frac{\partial u}{\partial y} = -\frac{1}{\rho}\frac{\partial p}{\partial x} + \nu\frac{\partial^2 u}{\partial y^2} \tag{1}$$

$$\frac{\partial v}{\partial t} = -\frac{1}{\rho}\frac{\partial p}{\partial y} \tag{2}$$

$$\frac{\partial v}{\partial y} = 0 \tag{3}$$

$$\rho C_p\left(\frac{\partial T}{\partial t} + v\frac{\partial T}{\partial y}\right) = \kappa\frac{\partial^2 T}{\partial y^2} + \mu\left(\frac{\partial u}{\partial y}\right)^2 \tag{4}$$

where (u,v) are the components of velocity in the (x,y) directions respectively, p is the pressure, ρ is the density, ν is the kinematic viscosity, t is the time, T is the temperature, κ is the thermal conductivity of the fluid and C_p is the specific heat at constant pressure.

Equation (3) suggests that v is independent of y and consequently it is a function of time only. We assume that

$$v = -V_0\left(1+\varepsilon A e^{\gamma t}\right) \tag{5}$$

where V_0 is the velocity of suction at the porous bed, γ is the accelerating factor and ε A is assumed to be very small quantity.

The boundary conditions are

$$\left.\begin{array}{l} \text{at} \quad y=0: \ \dfrac{\partial u}{\partial y} = \dfrac{\alpha}{\sqrt{K_0}}u \ , T = T_0 \\ \text{and as} \ \ y\to\infty : u \to U(t) \ , \ T \to T_\infty \end{array}\right\} \tag{6}$$

where U(t) is the free stream velocity , α is the dimensionless constant depending on the structure of the porous media and K_0 is the permeability of the porous medium.

The equation of the main stream is given by

$$-\frac{1}{\rho}\frac{\partial p}{\partial x} = \frac{dU(t)}{dt} \tag{7}$$

Using(7) in equation (1) , we have

$$\frac{\partial u}{\partial t} + v\frac{\partial u}{\partial y} = \frac{dU(t)}{dt} + \nu\frac{\partial^2 u}{\partial y^2} \tag{8}$$

We assume

$$U(t) = U_0\left(1+\varepsilon e^{\gamma t}\right) \tag{9}$$

$$u = U_0\left\{f_1(y) + \varepsilon f_2(y) e^{\gamma t}\right\} \tag{10}$$

where U_0 is the mean U(t) and ε may be taken as any positive quantity by suitable choice of origin.

We introduce the following non-dimensional quantities:

$$\eta = \frac{y|V_0|}{\nu} \ , \ \lambda = \frac{\nu\gamma}{V_0^2}, K^* = \frac{K_0}{\left(\dfrac{\nu}{V_0}\right)^2}, t^* = \frac{tV_0^2}{\nu}, \theta = \frac{T-T_\infty}{T_0-T_\infty} \tag{11}$$

We also assume that non-dimensional temperature θ is as follows:

$$\theta = \theta_1(\eta) + \varepsilon e^{\lambda t^*}\theta_2(\eta) + \varepsilon^2 e^{2\lambda t^*}\theta_3(\eta) \tag{12}$$

Using (5) and (9) to (12) in the equations (4) and (8) and comparing the co-efficients of various powers of $e^{\lambda t^*}$,we obtain

$$\frac{d^2 f_1}{d\eta^2} + \frac{df_1}{d\eta} = 0 \tag{13}$$

$$\frac{d^2 f_2}{d\eta^2} + \frac{df_2}{d\eta} - \lambda f_2 = -\lambda - A\frac{df_1}{d\eta} \tag{14}$$

$$\frac{d^2\theta_1}{d\eta^2} + \Pr\frac{d\theta_1}{d\eta} = -\mathrm{Br}\left(\frac{df_1}{d\eta}\right)^2 \tag{15}$$

$$\frac{d^2\theta_2}{d\eta^2} + \Pr\frac{d\theta_2}{d\eta} - \Pr\lambda\theta_2 = -A\Pr\frac{d\theta_1}{d\eta} - 2\mathrm{Br}\left(\frac{df_1}{d\eta}\right)\left(\frac{df_2}{d\eta}\right) \tag{16}$$

$$\frac{d^2\theta_3}{d\eta^2} + \Pr\frac{d\theta_3}{d\eta} - 2\Pr\lambda\theta_3 = -A\Pr\frac{d\theta_2}{d\eta} - \mathrm{Br}\left(\frac{df_2}{d\eta}\right)^2 \tag{17}$$

where

$$\Pr = \frac{\mu C_p}{\kappa}\,,\ \mathrm{Br} = \frac{\mu U_0^2}{\kappa\left(T_0 - T_\infty\right)}$$

are Prandtl number and Brinkmann number.

The corresponding boundary conditions are

$$\left.\begin{aligned} &\eta = 0: \frac{df_1}{d\eta} = \frac{\alpha}{\sqrt{K^*}} f_1, \frac{df_2}{d\eta} = \frac{\alpha}{\sqrt{K^*}} f_2, \theta_1 = 1, \theta_2 = 0 = \theta_2 \\ &\eta \to \infty: f_1 = 1 = f_2, \theta_1 = \theta_2 = \theta_3 = 0 \end{aligned}\right\} \tag{18}$$

On solving the boundary value problem (BVP) described by equations (13) to (18), we obtain

$$f_1 = 1 - \left(\frac{\alpha}{\alpha + \sqrt{K^*}}\right)e^{-\eta},$$

$$f_2 = 1 + \frac{A\alpha}{\lambda\left(\alpha + \sqrt{K^*}\right)} e^{-\eta} - \frac{2\alpha\left(A+\lambda\right)}{\lambda\left\{2\alpha + \sqrt{K^*}\left(1+\sqrt{1+4\lambda}\right)\right\}} e^{-\left(\frac{1+\sqrt{1+4\lambda}}{2}\right)\eta}$$

$$\theta_1 = e^{-Pr\,\eta} + \frac{Br\alpha^2}{\left(\alpha + \sqrt{K^*}\right)^2\left(4-2\,Pr\right)}\left(e^{-Pr\,\eta} - e^{-2\eta}\right),$$

$$\theta_2 = \left\{\frac{a_{11}}{Pr\,\lambda} - \frac{a_{12}}{\left(4-2\,Pr-Pr\,\lambda\right)} - \frac{a_{13}}{a_{14}}\right\} e^{-\left(\frac{Pr+\sqrt{Pr^2+4\lambda\,Pr}}{2}\right)\eta} - \frac{a_{11}}{Pr\,\lambda} e^{-Pr\,\eta} + \frac{a_{12}}{\left(4-2\,Pr-Pr\,\lambda\right)} e^{-2\eta} + \frac{a_{13}}{a_{14}} e^{-\left(\frac{3+\sqrt{1+4\lambda}}{2}\right)\eta}$$

$$\theta_3 = \left\{\frac{a_{15}}{Pr\,\lambda} - \frac{Aa_{11}}{2\lambda^2} - \frac{a_{18}}{\left(4-2\,Pr-2\,Pr\,\lambda\right)} - \frac{a_{16}}{a_{19}} - \frac{a_{17}}{a_{20}}\right\} e^{-\left(\frac{Pr+\sqrt{Pr^2+8\lambda\,Pr}}{2}\right)\eta} - \frac{a_{15}}{Pr\,\lambda} e^{-\left(\frac{Pr+\sqrt{Pr^2+4\lambda\,Pr}}{2}\right)\eta}$$

$$+ \frac{Aa_{11}}{2\lambda^2} e^{-Pr\,\eta} + \frac{a_{18}}{\left(4-2\,Pr-2\,Pr\,\lambda\right)} e^{-2\eta} + \frac{a_{16}}{a_{19}} e^{-\left(1+\sqrt{1+4\lambda}\right)\eta} + \frac{a_{17}}{a_{20}} e^{-\left(\frac{3+\sqrt{1+4\lambda}}{2}\right)\eta}$$

where the constants are given as

$$a_{11} = Pr^2\,A\left\{1 + \frac{Br\alpha^2}{\left(\alpha + \sqrt{K^*}\right)^2\left(4-2\,Pr\right)}\right\},$$

$$a_{12} = \frac{2Br\alpha^2 A}{\left(\alpha + \sqrt{K^*}\right)^2}\left\{\frac{1}{\lambda} - \frac{Pr}{\left(4-2\,Pr\right)}\right\},$$

$$a_{13} = -\frac{2Br\alpha^2\left(A+\lambda\right)\left(1+\sqrt{1+4\lambda}\right)}{\lambda\left(\alpha + \sqrt{K^*}\right)\left\{2\alpha + \sqrt{K^*}\left(1+\sqrt{1+4\lambda}\right)\right\}},$$

$$a_{14} = \left(\frac{3+\sqrt{1+4\lambda}}{2}\right)^2 - Pr\left(\frac{3+\sqrt{1+4\lambda}}{2}\right) - Pr\,\lambda\,,$$

$$a_{15} = A\,Pr\left\{\frac{a_{11}}{Pr\,\lambda} - \frac{a_{12}}{\left(4-2\,Pr-Pr\,\lambda\right)} - \frac{a_{13}}{a_{14}}\right\}\left(\frac{Pr+\sqrt{Pr^2+4\lambda\,Pr}}{2}\right),$$

$$a_{16} = -\frac{\left(\alpha+\sqrt{K^*}\right)^2 a_{13}^2}{4Br\alpha^2},$$

$$a_{17} = \frac{A\,Pr\,a_{13}}{a_{14}}\left(\frac{3+\sqrt{1+4\lambda}}{2}\right)+\frac{2BrA\alpha^2\left(A+\lambda\right)\left(1+\sqrt{1+4\lambda}\right)}{\lambda^2\left(\alpha+\sqrt{K^*}\right)\left\{2\alpha+\sqrt{K^*}\left(1+\sqrt{1+4\lambda}\right)\right\}},$$

$$a_{18} = \frac{2A\,Pr\,a_{12}}{\left(4-2\,Pr-Pr\,\lambda\right)}-\frac{BrA^2\alpha^2}{\lambda^2\left(\alpha+\sqrt{K^*}\right)^2},$$

$$a_{19} = \left(2-Pr\right)\left(1+2\lambda+\sqrt{1+4\lambda}\right),$$

$$a_{20} = \left(\frac{3+\sqrt{1+4\lambda}}{2}\right)^2 - Pr\left(\frac{3+\sqrt{1+4\lambda}}{2}\right)-2\lambda\,Pr\,.$$

3. Entropy analysis

The BVP as solved above provides velocity and the temperature fields which are readily utilized to compute entropy generation. The local volumetric rate of entropy generation S_G for the set up is given as follows.

$$S_G = \frac{\kappa}{T_\infty^2}\left(\frac{dT}{dy}\right)^2+\frac{\mu}{T_\infty}\left(\frac{du}{dy}\right)^2 \tag{19}$$

We see that two sources contribute in entropy generation. The first term accounts for the contribution of heat transfer to entropy and the second term is the local entropy generation due to dissipation.

In order to define the dimensionless entropy generation rate we prescribe the characteristic entropy generation rate S_{G0}, the dimensionless temperature difference ω and the non-dimensional number for entropy generation N_s respectively as follows

$$S_{G0} = \frac{\kappa\left(T_0-T_\infty\right)^2 V_0^2}{\left(\nu T_\infty\right)^2}\quad,\quad \omega = \frac{T_\infty}{T_0-T_\infty}\quad\text{and}\quad N_s = \frac{S_G}{S_{G0}}$$

$$N_s = \left(\frac{d\theta_1}{d\eta}+\varepsilon e^{\lambda t^*}\frac{d\theta_2}{d\eta}+\varepsilon^2 e^{2\lambda t^*}\frac{d\theta_3}{d\eta}\right)^2+Br\omega\left(\frac{df_1}{d\eta}+\varepsilon e^{\lambda t^*}\frac{df_2}{d\eta}\right)^2$$
$$= HTI + FFI$$

where

$$\text{HTI}= \left(\frac{d\theta_1}{d\eta} + \varepsilon e^{\lambda t^*} \frac{d\theta_2}{d\eta} + \varepsilon^2 e^{2\lambda t^*} \frac{d\theta_3}{d\eta} \right)^2 \text{ is heat transfer irreversibility}$$

and

$$\text{FFI}= \text{Br}\omega \left(\frac{df_1}{d\eta} + \varepsilon e^{\lambda t^*} \frac{df_2}{d\eta} \right)^2 \text{ is fluid friction irreversibility}$$

and the Bejan number is defined as

$$\text{Be} = \frac{\text{HTI}}{\text{HTI} + \text{FFI}}$$

$$= 1/(1+\text{FFI}/\text{HTI}) \qquad (20)$$

4. Results and Discussion

The figures 1-6 and figures 7-12 display variations in entropy generation number N_s and Bejan number Be respectively. Figure-1 displays that the slip coefficient α has qualitative effect on entropy generation number N_s. We see that the N_s rises with increasing values of α. This makes a point recalling the fact that the slip coefficient α may have different values for the porous medium without compromising the permeability or bulk porosity. That is, α depends on non-uniformities in the arrangement of solid material at the surface, hence materials having same permeability or same bulk porosity exhibit different values of α. This leads us to conclude that entropy generation may be managed by adjusting values of α without compromising the permeability of the permeable base. Hence, slip coefficient can serve as a pertinent entropy controlling parameter in thermal system of interest. Furthermore, the figures reveal that entropy undergoes qualitative and quantitative variations adjacent to the permeable wall where a suction has been applied and there is hydrodynamic slip as well. It is also seen that there is an asymptotic decay in entropy far away from the permeable base.

Figure-2 exhibits that entropy generation number rises with increasing values of Brinkman number Br. Figure-3 displays that N_s decreases with increasing values of permeability. Figure-4 displays that entropy generation number increases with increasing values of suction parameter λ. Figure-5 reveals that N_s increases with increasing values of characteristic temperature ratio ω. Figure-6 reveals that N_s registers considerable increase as time elapses.

The figures 7-12 reveal that Bejan number attains minima at different spatial distances y for different sets of parameter values. Further, we observe that Be is larger at the distances far away from the permeable base. This means that FFI/HTI is larger at the permeable surface as compared to that at far away distances from the permeable surface.

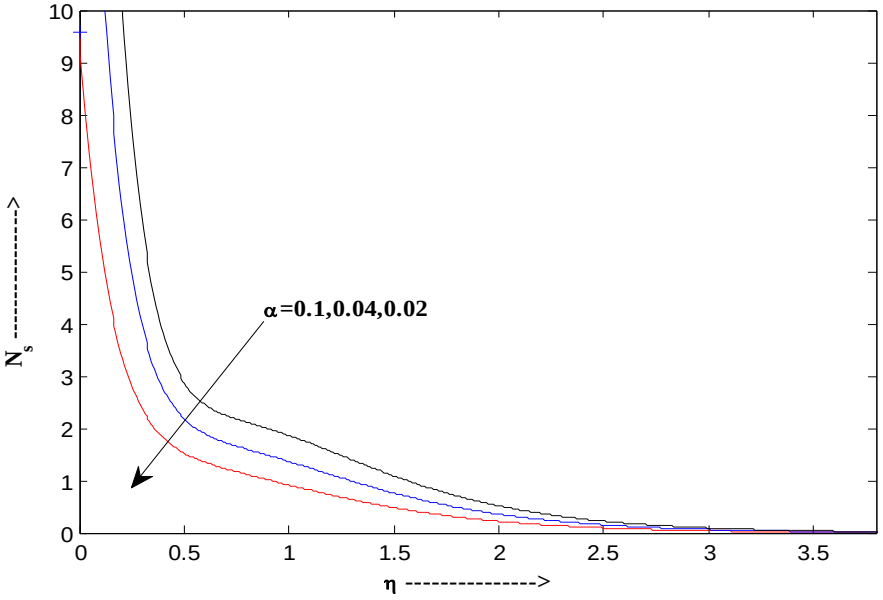

Figure 1: Entropy variation for varying α, for ε=0.05, A=0.1,t*=1,K*=0.0001,λ=1.5, Pr=0.9,ω=0.6,Br=10

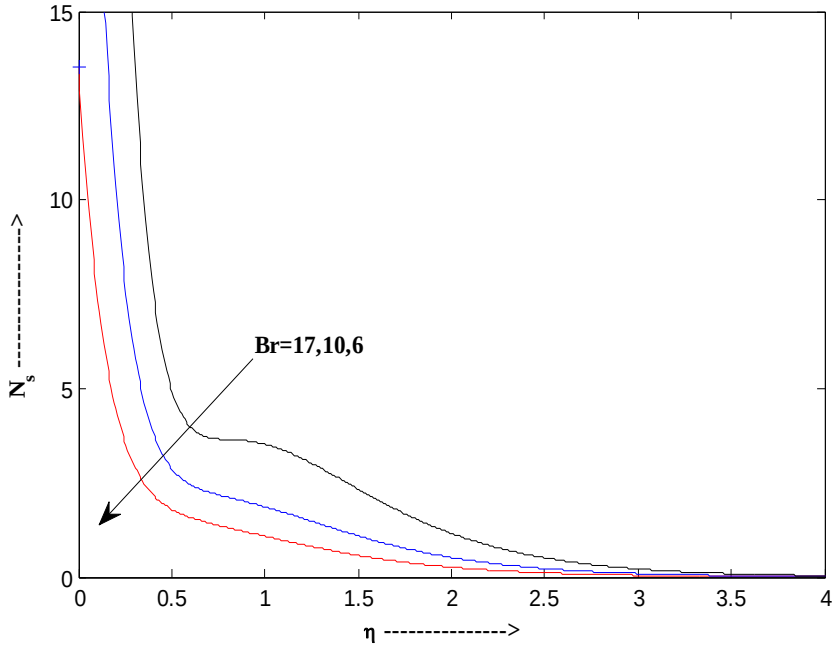

Figure 2: Entropy variation for varying Br, for ε=0.05,A=0.1,α=0.1,t*=1,K*=0.0001,λ=1.5, Pr=0.9,ω=0.6

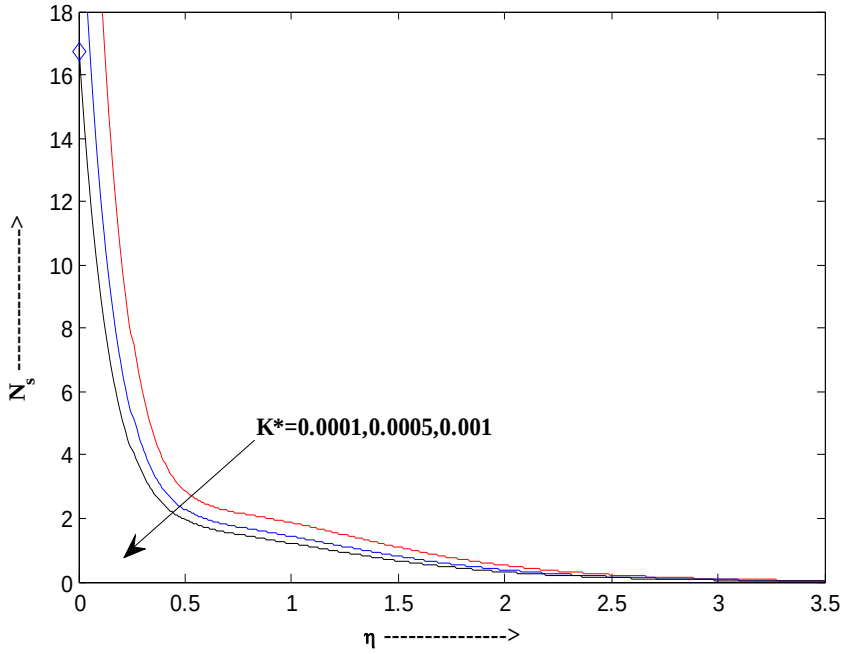

Figure 3: Entropy variation for varying K*, for ε=0.05,A=0.1,α=0.1,t*=1,λ=1.5, Pr=0.9,ω=0.6,Br=10

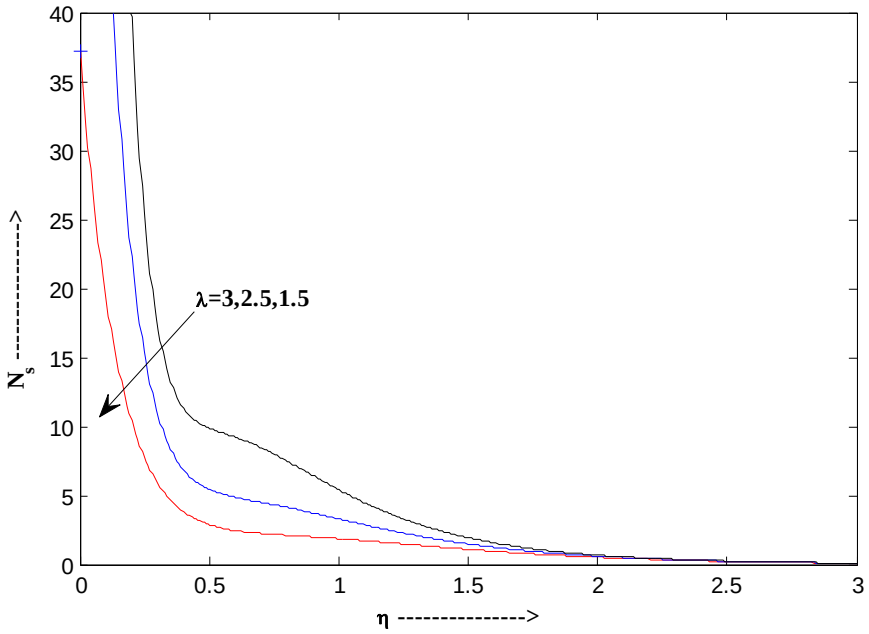

Figure 4: Entropy variation for varying λ, for ε=0.05, A=0.1,α=0.1,t*=1,K*=0.0001,Pr=0.9,ω=0.6,Br=10

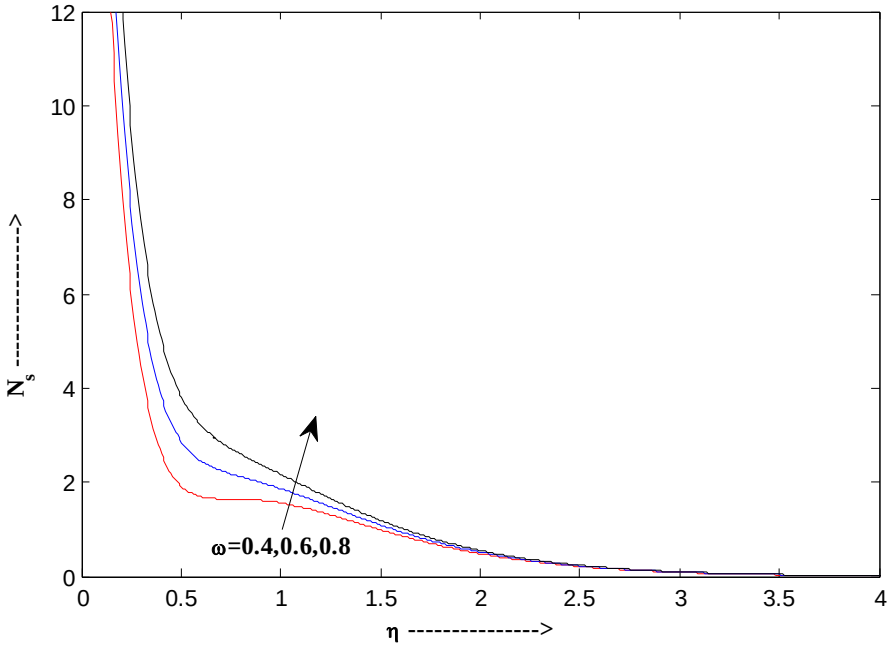

Figure 5: Entropy variation for varying ω, for ε=0.05,A=0.1,α=0.1,t*=1,K*=0.0001,λ=1.5, Pr=0.9,Br=10

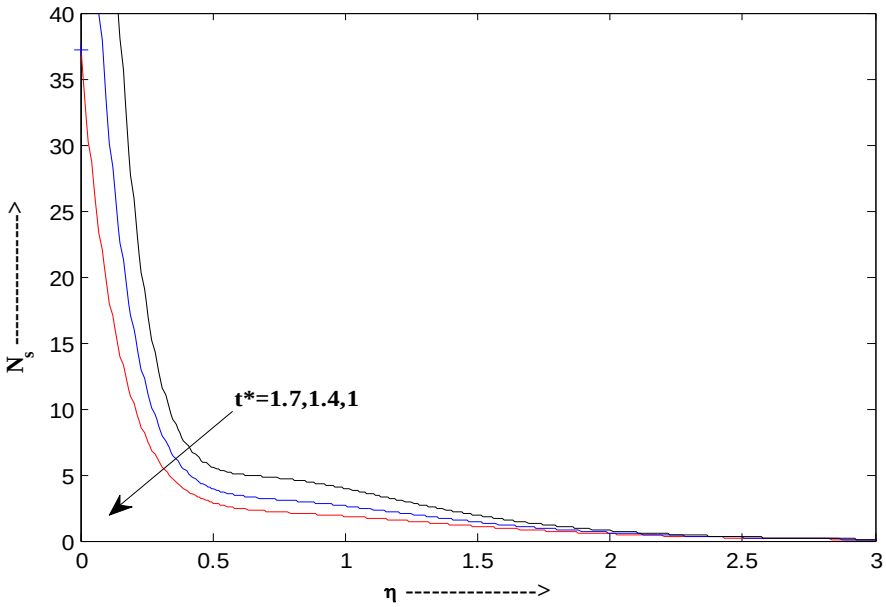

Figure 6: Entropy variation for varying t*, for ε=0.05, A=0.1,α=0.1,K*=0.0001,λ=1.5,Pr=0.9,ω=0.6,Br=10

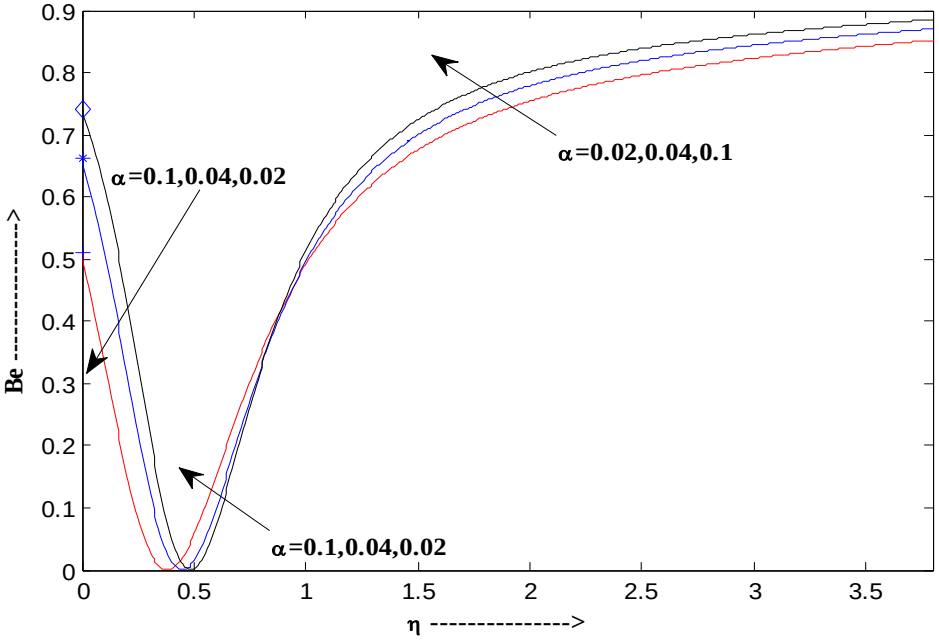

Figure 7: Bejan number variation for varying α, for ε=0.05,A=0.1,t*=1,K*=0.0001,λ=1.5,Pr=0.9,ω=0.6,Br=10

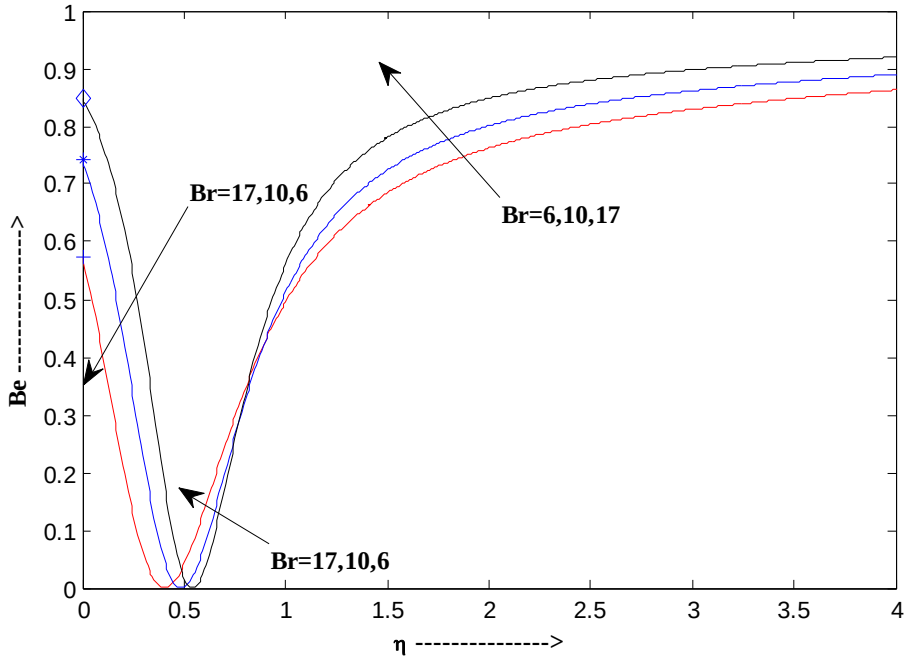

Figure 8: Bejan number variation for varying Br, for ε=0.05,A=0.1,α=0.1,t*=1,K*=0.0001,λ=1.5, Pr=0.9,ω=0.6

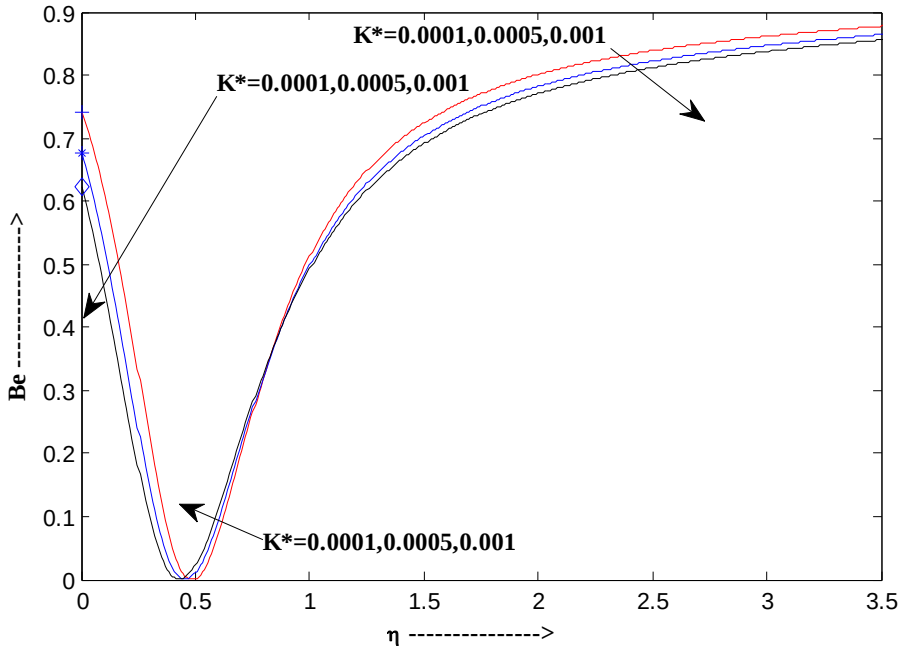

Figure 9: Bejan number variation for varying K*, for ε=0.05,A=0.1,α=0.1,t*=1,λ=1.5, Pr=0.9,ω=0.6,Br=10

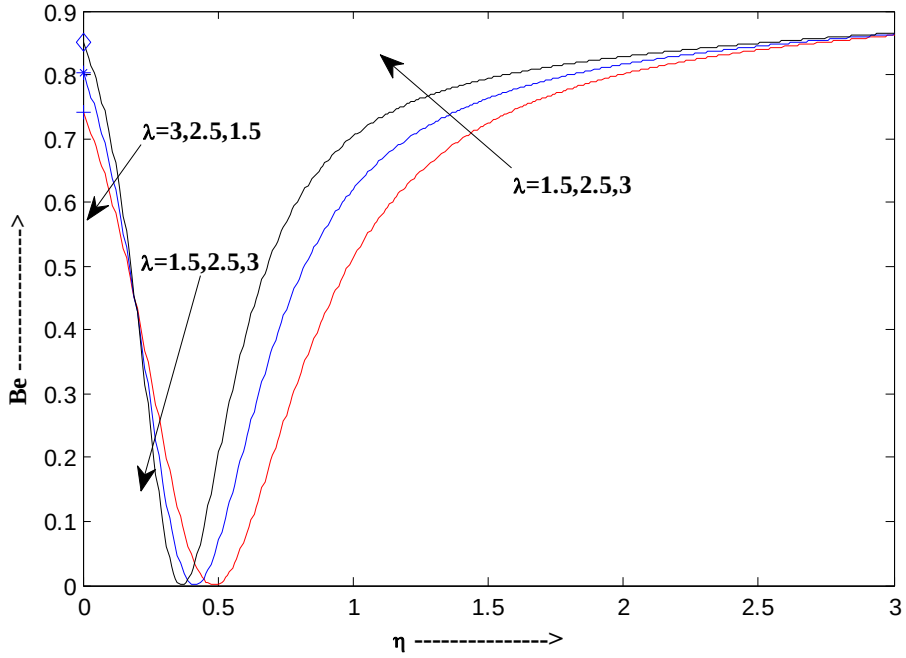

Figure 10: Bejan number variation for varying λ,for ε=0.05,A=0.1,α=0.1,t*=1,K*=0.0001,Pr=0.9,ω=0.6,Br=10

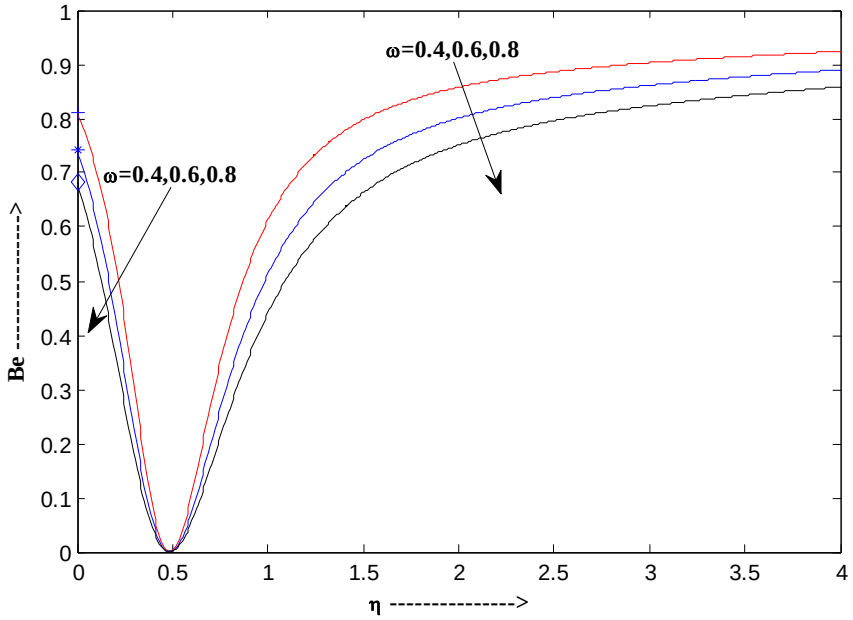

Figure 11: Bejan number variation for varying ω, for ε=0.05,A=0.1,α=0.1,t*=1,K*=0.0001,λ=1.5, Pr=0.9,Br=10

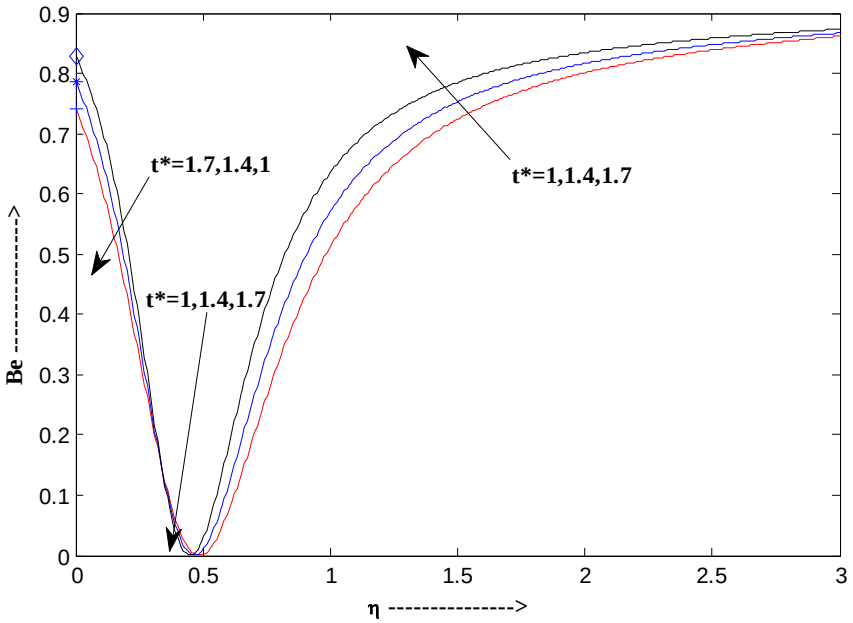

Figure 12: Bejan number variation for varying t*, for ε=0.05,A=0.1,α=0.1,K*=0.0001,λ=1.5, Pr=0.9,ω=0.6,Br=10

5. References

[1] Bejan, A. (1996). *Entropy Generation Minimization*, CRC: Boca Raton, NY, USA.

[2] Bejan, A. (2002). Fundamentals of energy analysis, entropy generation minimization, and the generation of flow architecture. *Int. J. Energy Res*.,Vol. 26, 545–565.

[3] Bejan, A. (1982). Second-law analysis in heat transfer and thermal design, Adv. *Heat Transf*., Vol. 15, pp.1–58.

[4] Chauhan, D.S. and Vyas, P. (1995). Heat transfer in hydromagnetic couette flow of compressible Newtonian fluid, *ASCE Journal of Engineering Mechanics*, Vol.121, pp.57-61.

[5] Chauhan, D.S. and Khemchandani, V. (2016). Entropy Analysis of a Coupled-Convection Flow through a Vertical Channel Partially Filled by a Porous Medium with Injection/Suction and Slip Boundary Conditions, *Heat transfer*, DOI: 10.1002/htj.21252.

[6] Chauhan, D.S. and Kumar, V. (2013). Entropy analysis for third-grade fluid flow with temperature-dependent viscosity in annulus partially filled with porous medium, *Theoret.Appl.Mech*. Vol.40, No.3, pp.441-464, Belgrade.

[7] Chauhan, D.S. and Sahai, S. (2005). Flow and Heat transfer over a naturally permeable bed of very small permeability with a variable suction, *Int. J. Theor. Phys*. Vol. 53, No.2, pp.151-159.

[8] Darcy, H. (1856), *Les Fontanies Publiques de la Ville de Dijon*, Dalmont, Paris.

[9] Fowler A.J. and Bejan A. (1995). Forced convection from a surface covered with flexible fibres, *Int. J. Heat Mass Transfer*, Vol.38, pp.767-777.

[10] Hooman, K. and Ejlali, A. (2007). Entropy generation for forced convection in a porous saturated circular tube with uniform wall temperature, *Int. Commn. Heat Mass transfer*, Vol.34, 408-419.

[11] Huang, P.C. and Vafai, K. (1993). Flow and heat transfer control over an external surface using a porous block arrangement, *Int. J. Heat Mass Transfer*, Vol.36, pp.4019-4032.

[12] Huang, P.C. and Vafai, K. (1994). Passive alteration and control of convective heat transfer utilizing alternate porous cavity-block wafers, *Int. J. Heat Fluid Flow*, Vol.15, pp.48-61.

[13] Ibanez, G. (2015). Entropy generation in MHD porous channel with hydrodynamic slip and convective boundary condition. *Int. J. Heat Mass Transfer* Vol.80, 274-280.

[14] Ibanez, G.; Lopez, A.; Pantoja J. Moreira, J. and Reyes, J.A. (2013). Optimum slip flow based on the minimization of entropy generation in parallel plate microchannels, *Energy*, Vol.50, 143-149.

[15] Ibanez, G.; Lopez, A.; Pantoja J. and Moreira, J. (2014). Combined effects of uniform heat flux boundary conditions and hydrodynamic slip on entropy generation in a microchannel, *Int. J. Heat Mass Transfer*, Vol.73, 201-206.

[16] Mahmud, S. and Fraser, R.A. (2005). Flow, thermal and Entropy generation characterises inside a porous channel with viscous dissipation, *Int. J. Thermal science*, Vol.44, 21-32.

[17] Makinde O.D. and Eegunjobi, A.S. (2013). Effects of convective heating on entropy generation rate in a channel with permeable walls, *Entropy* 15(1), 220-233.

[18] Saffman, P.G. (1971). On the boundary condition at the surface of a porous medium, *Stud. Appl. Math*, Vol.2, pp.93-101.

[19] Vafai, K. and Kim, S.J. (1990). Analysis of surface enhancement by a porous substrate, *ASME J. Heat transfer*, Vol.112, pp.700-706.

[20] Vyas, P. and Srivastava, N.(2015). Entropy analysis of generalized MHD Couette flow inside a composite duct with asymmetric convective cooling., *Arabian J. for Science and Engineering* Vol.40,No.2, 603-614.

[21] Vyas , P. and Srivastava, N. (2014). Radiative MHD compressible Couette flow in a parallel channel with a naturally permeable wall, *Thermal Science* Vol.18 (suppl.2):573-585. DOI:10.2298/TSCI120828099V.

[22] Vyas, P. and Khan, S. (2016). Entropy analysis for MHD dissipative Casson fluid flow in porous medium due to stretching cylinder, *Acta Technica*, Vol.61, No.3, pp299-315.

[23] Vyas, P. and Rai, A. (2013). Entropy regime for radiative MHD Coutte flow inside a channel with naturally permeable base, *Int. J. Energy Technol*. Vol.5, 1-9.

[24] Vyas, P. and Ranjan, A. (2015). Entropy analysis of radiative MHD forced convection flow with weakly temperature dependent convection coefficient in porous medium channel, *Acta Technica*, Vol.60, No., pp. 1-14.